International Tables for Crystallography (2012). Vol. F, Section 9.1.10, pp. 222–223.

much, and the signal-to-noise ratio is enhanced at longer distances. It is advantageous to use the largest possible CTDD under the condition that meaningful data extend to, but not beyond, the active edge of the detector.

It is not straightforward to judge the resolution limit of meaningful diffraction. The most scientific approach involves recording, processing and merging a small number of images and making a decision on the basis of the resulting intensity statistics. However, this does require time, which should only pose a problem on ultra-high-intensity sources with very rapid data collection. A more pragmatic approach relies on visual inspection of the initial exposures using a graphical display at various contrast levels. Normally, if reflections are not visible by eye at the highest display contrast, their intensities are not meaningful. Some safety margin can be applied by setting the CTDD to a slightly shorter value than that estimated from visual inspection. Naturally, the resolution limit to which meaningful intensities extend depends on the exposure time, and the decision concerning the CTDD should follow the selection of the appropriate exposure (Section 9.1.11.2).

In addition to the significance of the reflection intensities, another important factor is the spatial resolution of spot profiles on the detector. If the crystal cell dimensions are large, the profiles may superimpose and the reflections may be impossible to integrate. At longer CTDD, the diffraction pattern spreads out and the profile overlap diminishes. If necessary, the detector can be offset from the central position to measure high-resolution data at long CTDD, but a larger total rotation is required to reach full data completeness. This applies only if the overlap of profiles belonging to the same lune results from a long axis lying parallel to the detector plane. The superposition of reflection profiles resulting from overlapping lunes will not be alleviated by increasing the CTDD; the only remedy for this is to reduce the rotation range $\Delta\varphi$ per exposure.

In addition to the proper selection of the CTDD, attention should be paid to the proper positioning of the beam stop. It should be centred with respect to the direct beam and cover the beam cross section completely. No part of the direct beam should reach the detector, and there should be no indirect scatter by the beam stop. The optimal reduction of air scatter is to have the smallest beam stop consistent with the dimensions of the beam, placed as close to the crystal as possible. For a given size of beam stop, the crystal-to-beam stop distance should be matched to the CTDD, sufficiently far from the crystal to minimize its shadow and concomitant obstruction of the valuable lowest-resolution reflections. If the beam stop is mounted on a metal wire, it is better to position the wire along the spindle axis where it will only interfere with those reflections around the blind region.

9.1.9. Wavelength

The wavelength of X-radiation can be tuned only at synchrotron sources. Rotating-anode generators produce radiation at a fixed wavelength which is characteristic of the metal of the anode, usually copper with $\lambda = 1.542$ Å.

The proper selection of the wavelength is most important for collecting data containing an anomalous-scattering signal. In general, the imaginary component $\Delta f''$ of the anomalous-dispersion signal is high on the short-wavelength side of the absorption edge of the anomalous scatterer present in the crystal. Near the absorption edge, both components, real $\Delta f'$ and imaginary $\Delta f''$, vary significantly. This variation is utilized in the MAD technique, the strict requirements of which are discussed in Chapters 14.2 and 14.3.

If the data are collected using a single wavelength with the aim of measuring Bijvoet differences, $\Delta F_{\rm anom} = F^{+} - F^{-}$, the requirements are not as strict as for MAD. However, it may be advisable to record the fluorescence spectrum around the region of the expected absorption edge. If the fluorescence signal from the crystalline sample is too weak, the appropriate metal or salt standard can be used. When using anomalous scatterers displaying large white lines within their spectra, the wavelength should be accurately adjusted on the basis of the spectrum measured from the actual sample.

For collecting data without an anomalous signal, there are no strict requirements concerning the wavelength. The maximum intensity provided by the beamline depends on the energy of particles in the synchrotron storage ring and on the beamline optics. Typically, wavelengths around 1 Å or shorter are used at most synchrotrons, assuring high beam intensity and low absorption of X-rays by the sample and air, thus reducing the radiation damage of the crystal. This is of particular importance at the very bright beamlines at third-generation synchrotrons. To diminish the effect of air absorption further, it is possible to fill the space between the crystal and the detector with helium. Short wavelengths are advantageous for collecting high-resolution data, since the diffraction angles are smaller and there is no need to use a very short CTDD. The effect of profile elongation owing to the oblique incidence of diffracted X-ray beams on the detector is then smaller, and the blind region is narrower.

9.1.10. Lysozyme as an example

Tetragonal hen egg-white lysozyme (Chapter 25.1 and Blake *et al.*, 1967), crystallizing in the space group $P4_32_12$ with cell dimensions $a = b = 78.6$ and $c = 37.2$ Å, is used here as a model system to illustrate some of the points made above, based on Dauter (1999). The example involves a set of two consecutive blocks of images with a crystal-to-detector distance of 243 mm, a wavelength of 0.92 Å, a resolution of 2.7 Å, an oscillation range of 1.5° and a crystal mosaicity around 0.5°. These images are shown in Fig. 9.1.10.1(*a*–*f*).

The first four images, (*a*–*d*), were exposed with the tetragonal fourfold *c* axis lying approximately along the direction of the beam. On these images, the reflections within each lune are arranged in a square grid, reflecting the tetragonal symmetry with $a = b$. The squares are oriented with their diagonals in the horizontal and vertical directions of the image, as the crystal was mounted with its [110] direction along the spindle rotation axis. Indeed, at the end of image (*a*) and the start of image (*b*), the *c* axis lay almost perfectly along the beam, and the zero-layer lune almost disappears behind the beam-stop shadow, since the corresponding (*hk*0) plane in reciprocal space is tangential to the Ewald sphere at the origin of the reciprocal lattice.

The lunes are widely spaced with clear gaps between them, because the third cell dimension, *c*, which is perpendicular to the detector plane, is relatively short, 37.2 Å. Images (*e*–*f*), exposed at an angle on the rotation spindle roughly 90° away from (*a*–*d*), have a quite different appearance, despite the rotation range per image being the same. Each lune is less densely populated by reflections, but the number of lunes is larger and the gaps between them much smaller. This arises from the lunes now being parallel to the (*hhl*) family of planes, as the $[1\bar{1}0]$ vector is now parallel to the beam. The interplanar spacing within this family is less than for those on images (*a*–*d*), hence at high resolution,

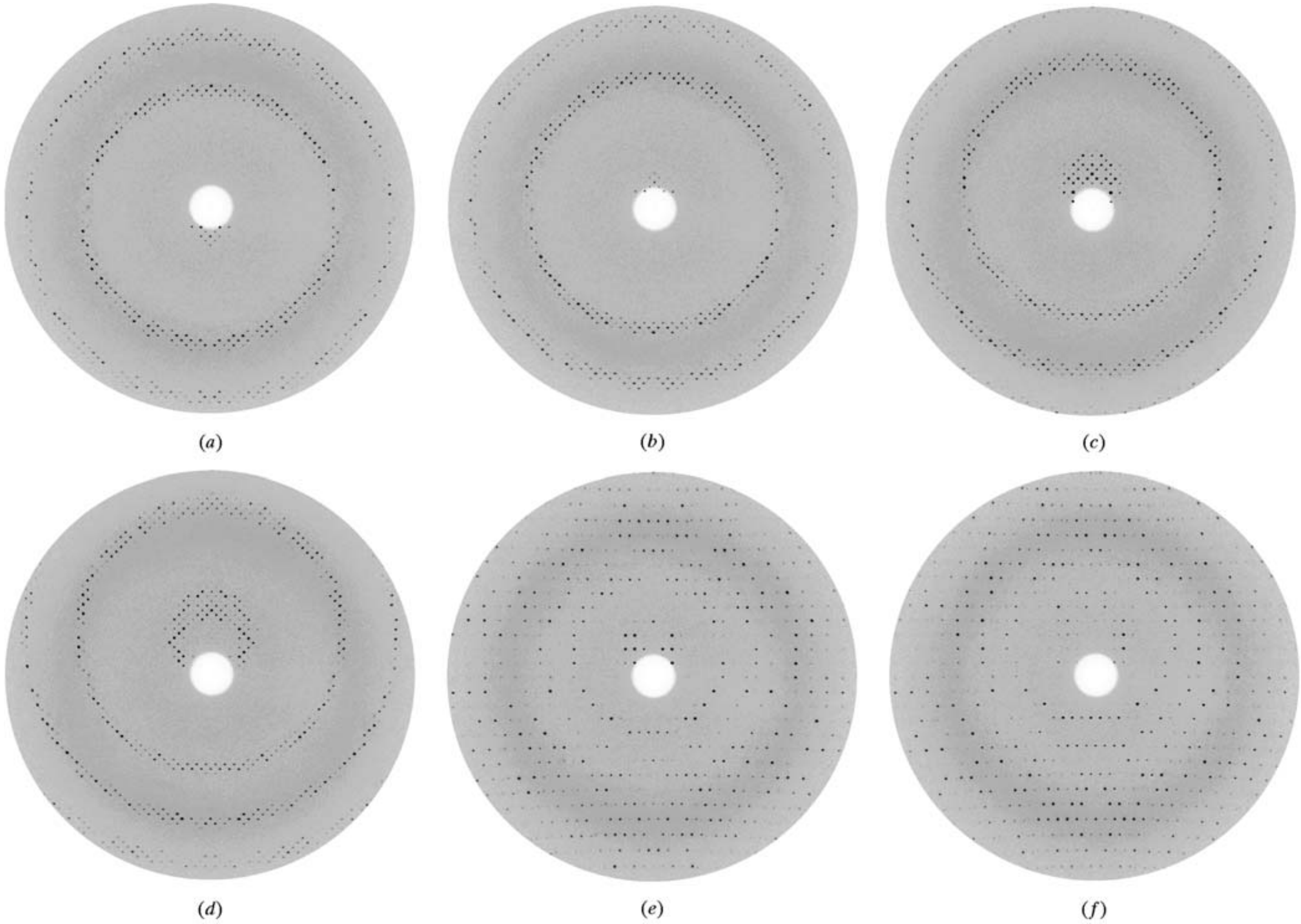

Figure 9.1.10.1
Images recorded from a crystal of lysozyme. (*a–d*) Four consecutive exposures with the crystal fourfold axis parallel to the X-ray beam. (*e–f*) Two successive exposures 90° away, when the fourfold axis lies vertically in the plane of the image. The crystal [110] direction is parallel to the rotation axis, horizontal in the plane of the images.

close to the edge of the detector window, the lunes overlap on images (*e–f*). The reflections, however, do not overlap, as the crystal orientation is diagonal; the lunes are sparsely populated, with large separation between adjacent spots, so the reflections on successive lunes fit between one another. It should be noted that the density of reflections in different regions of the reciprocal lattice is constant, and that the total number of reflections recorded on an image depends only on the rotation range, not on the crystal orientation.

The zero-layer lune containing reflections with indices $hk0$ is especially evident on exposures (*c–d*) directly above the centre of the image. With such a lune close to the centre, the reciprocal lattice shows minimal distortion owing to its projection onto the detector plane, and the lune appears as a 'pseudo-precession' pattern. The systematic absence of every second reflection, with odd index, along the $h00$ and $0k0$ lines indicates the presence of twofold screw axes of symmetry along the crystal axes *a* and *b*. Images (*e–f*), 90° away, have the hhl lune at the centre and, although it is less well separated from higher lunes, the presence of a fourfold screw axis along **c** is confirmed by the presence of only every fourth reflection on the $00l$ line. This allows the identification of the space group as $P4_12_12$ or its enantiomorph, $P4_32_12$. In general, the positions of the reflections define only the Bravais lattice, and it is the symmetry of the intensity pattern which reflects the point group. Thus, further confirmation that the symmetry belongs to point group $P422$ rather than $P4$ comes from the symmetric relation of the intensity distribution on either side of each lune in images (*a–d*). This is equivalent to the earlier use of precession photography for space-group elucidation.

Close inspection shows that the reflections at the edges of the lune are also present on the adjacent image. The rotation range was 1.5°, and the mosaicity was estimated at 0.5°, and thus about one-sixth of the reflections are partially recorded at each edge of the lune, giving one-third partially recorded terms in total. The lack of sharpness at the edge of the lunes confirms a substantial level of mosaicity.

9.1.11. Rotation method: qualitative factors

9.1.11.1. Inspection of reflection profiles

Reflection profiles should be checked on the first recorded images. Very often a quick inspection of the profiles can disqualify a bad crystal without further loss of time. The profiles should have a single maximum and smooth shoulders. If the crystal shape is irregular, it may be reflected in the spot profile. Profiles should not have double maxima or be substantially elongated or smeared out, which usually arises from crystal splitting. The profiles should certainly be inspected if initial autoindexing of the diffraction pattern is unsuccessful.

Even if the spot profiles appear to be regular on the first image, it is good practice to inspect a second image at a substantially different φ rotation angle, preferably 90° away, since crystal splitting may have a similar effect on the appearance of the lunes and profiles as does high mosaicity on a single image (Section